Thermodynamics and Molecular Mechanics Studies on α- and β-Cyclodextrins Complexation and Diethyl 2,6-naphthalenedicarboxylate Guest in Aqueous Medium

Isabel Pastor, Antonio Di Marino, and Francisco Mendicuti*

Departamento de Química Física, Universidad de Alcalá, 28871 Alcalá de Henares, Madrid, Spain

Received: August 10, 2001; In Final Form: November 6, 2001

Steady-state, time-resolved fluorescence spectroscopy and Molecular Mechanics (MM) were used to study the inclusion complexes of Diethyl 2,6-naphthalenedicarboxylate (DEN) with α- and β-cyclodextrins (CDs). The ratio, *R*, of intensities of two bands that are sensitive to the medium polarity and the average of lifetime, $<\tau>$, which is more sensitive to the medium microviscosity surrounding the guest molecule, were obtained as a function of the CD concentration and temperature. Stoichiometries, formation constants, and the changes of enthalpy and entropy upon inclusion were also obtained. The complexes prefer 1:2 (DEN:CD) stoichiometries. MM calculations were employed to study the formation of different complexes of DEN with both α- and βCDs. For the most stable structure of 1:1 complexes, an important portion of DEN is outside CD cavity, making it possible to stabilize them by adding another CD. Driving forces for 1:2 inclusion processes are dominated by nonbonded van der Waals DEN−CD interactions. Nevertheless, due to the different geometry of the 1:2 complexes, an important electrostatic interaction appears between both βCDs in the DEN:βCD_2 complex that does not exist between αCDs in the DEN:αCD_2 complex. Most of this contribution is due to the intermolecular hydrogen bonding formation between secondary hydroxyl groups of both βCDs.

1. Introduction

Cyclodextrins (CDs) are cyclic torus-shaped molecules made up of the α-1,4 linkages of glucopiranose units. These compounds are known for their ability to form inclusion complexes with low molecular weight compounds and polymers giving interesting supramolecular assemblies.[1−4] Due to their particular characteristics, complexation depends mainly on the size, shape, and polarity of the guest molecule relative to the CD low polar inner cavity. When the guest contains a chromophore, fluorescence spectroscopy[5−29] can be a useful tool for obtaining stoichiometry, information on the geometry of the complex, association constants, and the thermodynamic parameters accompanying the complexation process. Some of the steady-state fluorescence techniques used include enhancement or quenching of the emission,[5−15] excimer formation,[16−20] fluorescence depolarization,[21] or finding the relative intensity of some vibronic bands of the emission spectrum upon inclusion.[5,23,24,30] However, time-resolved fluorescence measurements have been used less frequently for these purposes.[10,15,22,23] Molecular Modeling[31,32] can also strengthen experimental results providing information on the driving forces responsible for complexation processes.

We have been using Molecular Mechanics (MM) and Molecular Dynamics (MD) to study the inclusion phenomena of small and large molecules[33−41] with CDs. One of our latest studies was done on the complexation of Dimethyl 2,6-naphthalenedicarboxylate (DMN) with α- and βCDs.[41] DMN emission spectra showed two bands whose ratio of intensities, *R*, was very sensitive to medium polarity. From the variation of *R* with the CD concentration and temperature, the association constants, stoichiometries, and enthalpy and entropy changes upon complexation were obtained. DMN forms complexes of stoichiometries 1:2 and 1:1 with α- and βCD, respectively. The estimated association constants at 25 °C were relatively large, $\sim 8 \times 10^5\ M^{-2}$ and $\sim 1.3 \times 10^3\ M^{-1}$ for DMN:αCD_2 and DMN:βCD, respectively. A dependence of $\Delta H°$ and $\Delta S°$ on temperature with a negative value of ΔC_p^0 was observed for both complexes. DMN complexation with two αCD was accompanied by larger negative enthalpy and entropy changes than the formation of the DMN:βCD complex, which was even followed by an entropy increase. MM studies on both 1:1 and 1:2 complexes in the presence of water showed that only a small portion of DMN penetrates into the αCD, but that it does so almost totally into the βCD cavity. A stabilization, where van der Waals interactions dominate, takes place when another CD approaches to the DMN:αCD complex. This hardly happens with the DMN:βCD complex. Hydrogen bonding between secondary hydroxyl groups of αCD also contributes to the stability of the 1:2 complex.

2. Experimental Section

2.1. Materials. Diethyl 2,6-naphthalenedicarboxylate (DEN) was obtained by reaction of 2,6-naphthalenedicarboxylic acid chloride with ethanol in the presence of triethylamine. Previously, diacid chloride was prepared from the commercial 2,6-naphthalenedicarboxylic acid (Aldrich) by reaction with an excess of thionyl choride (Aldrich). More details for synthesis of similar compounds were previously reported.[42] Purification was achieved by recrystallization (×3) from the chloroform solutions by adding a slight amount of methanol. DEN was characterized by NMR. α- and βCD used were Aldrich. The αCD was used as purchased, and the βCD was recrystallized (×2) from water (Milli-Q). TGA reveals a water by mass content of ∼10% and ∼6% for the α- and βCD, respectively. Methanol, ethanol, ethylene glycol (Aldrich, spectrophotometric grade) and Milli-Q water solvents were checked by fluorescence before using. DEN/CD water solutions were prepared by weight from

* To whom correspondence should be addressed, Phone: 34-91-8854672. Fax: 34-91-8854763. E-mail: francisco.mendicuti@uah.es.

10.1021/jp013118q CCC: $22.00
Published on Web 02/01/2002

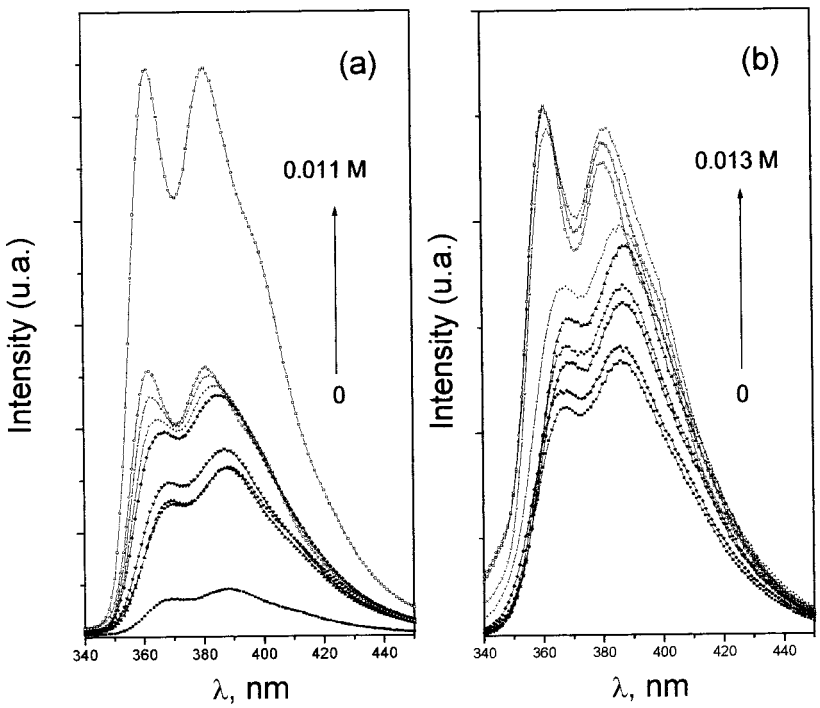

Figure 1. Uncorrected emission spectra of DEN aerated aqueous solutions and at different CD concentrations at 25 °C upon λ_{exc}=294 nm. (a) [αCD]= 0; 0.001 02 M; 0.002 10 M; 0.003 91 M; 0.005 01 M; 0.007 14 M; 0.008 52 M; 0.009 82 M; and 0.0110 M. (b) [βCD]= 0; 0.000 59 M; 0.000 90 M; 0.001 25 M; 0.002 30 M; 0.004 55 M; 0.00743 M; 0.0010 M; and 0.0130 M. The [DEN] was held constant.

a double filtered (0.45 μm diameter size cellulose Millipore filters) aqueous DEN saturated solution ($\sim 10^{-6}$ M) as described previously.[41] Prior to measuring, all solutions were stirred for about 2 d. Concentrations of α- and βCD ranged from 0 to approximately $1.0-1.3 \times 10^{-2}$ M. DEN concentration was held constant in all experiments.

2.2. Apparatus. Steady-state fluorescence measurements were performed by using an SLM 8100 AMINCO spectrofluorimeter. The SLM 8100 is equipped with polarizers, a double (single) concave grating monochromator in the excitation (emission) path, and a cooled photomultiplier. Slit widths were set at 8 nm for excitation and emission and polarizers at the magic angle. Fluorescence decay measurements were performed on a time-correlated single-photon-counting FL900 Edinburgh Instruments Spectrometer. Due to the low DEN concentration and fluorescence signal, the thyratron-gated lamp (nF900) was filled with nitrogen. Concave gratings monochromators were used at the excitation and emission paths with slits set to18 nm. Photons were detected by a red sensitive cooled photomultiplier. The data acquisition was carried out by using 1024 channels of the multichannel analyzer with a time window width of 250 ns. A total of 5000 counts in the peak channel were taken for each measurement. Instrumental response functions were regularly achieved by measuring the scattering of a Ludox solution and the quality of the fit was judged by the reduced χ^2 criterion, the inspection of the weighted residuals per channel and the autocorrelation function of the weighted residuals. Decay profiles were fitted to multiexponential trail functions by the iterative reconvolution method.[43]

Emission spectra were obtained upon 294 nm as excitation wavelength. Decay profiles were obtained by exciting at 296 nm, one of the peaks of the spectral output of the N_2 lamp, and selecting the emission at 385 nm. Measurements of different solutions were performed in the range of temperatures from 5 to 45 °C at 10 °C intervals (Techne RB-5, TE−8A).

2.3. Experimental Results. *2.3.1. Steady-State Fluorescence.* Figure 1 depicts the uncorrected emission spectra of DEN water solutions in the absence and presence of different concentrations of αCD (a) or βCD (b) at 25 °C. As the CD concentration increases, the fluorescence intensity increases drastically for DEN/αCD solutions, this increase, however, is smaller for DEN/βCD solutions. No isosbestics points are clearly detected. Both spectra are very similar to those reported for DMN water solutions with both CDs,[41] i.e., two main overlapping bands centered in the range 362−9 nm and 383−8 nm. The location of the maxima of these bands also change slightly upon the addition of CD toward the low limit of each range. But the main feature is the change in the relative intensity of both bands with CD concentration and temperature. The parameter R defined as the ratio of intensities at the wavelengths of the maximum of both peaks, $R = \{I_{\sim 385nm}\}/\{I_{\sim 365nm}\}$, used previously with other similar guests,[33,36,41] represents a quantitative measure of the change. The upper part of Figure 2 depicts the variation of R with CD concentration for the DEN/CD solutions at different temperatures. Upon addition of CD the ratio R monotonically decreases. The amount of this decrease, however, depends on the type of CD used and on the temperature. The lower value of R with CD added at each temperature should infer that more DENs are complexed. The same effect was observed with other guest molecules, including DMN.[41] The fact (a) that higher CD concentrations than those used in our measurements at any temperature are required to reach the constant plateau, suggests relatively low association constants for these complexes. Also, the fact (b) that, at a given CD concentration, higher values of R are obtained with temperature, suggests a decrease in complex stability as the temperature increases ($\Delta H < 0$). There is no evidence of the presence of DEN excimers that could imply the possibility of more than one DEN penetrating into the CD cavity.

2.3.2. Fluorescence Intensity Decays. Fluorescence intensity decays for DEN solutions in the absence and presence of CD at different temperatures were also performed. For a particular sample, the shape of the decays does not change noticeably upon changing the emission wavelength. The decay profiles for DEN

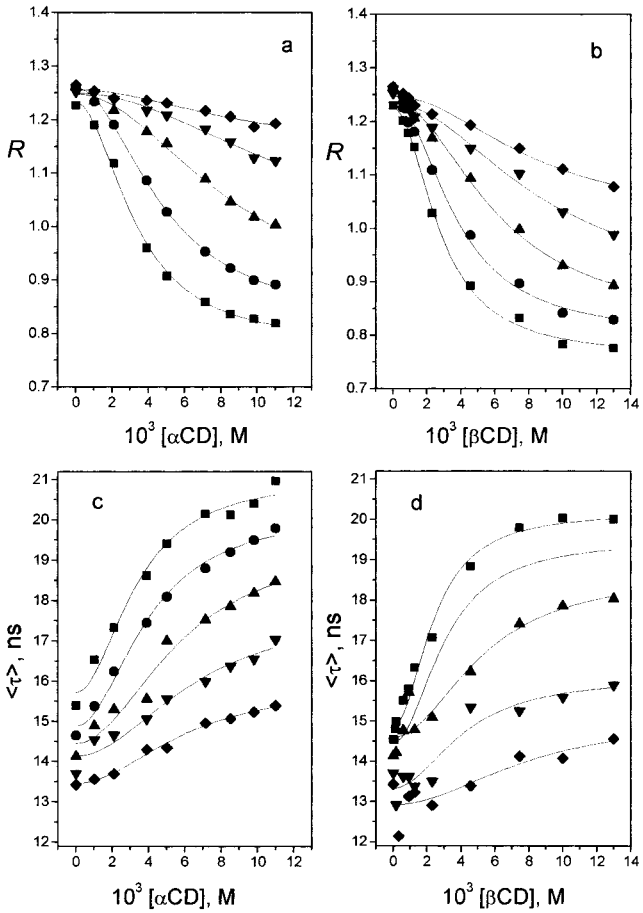

Figure 2. Variation of R and average of lifetime $<\tau>$ with [αCD] (a, c) and [βCD] (b,d) at different temperatures, 5 °C (■); 15 °C (●); 25 °C (▲); 35 °C (▼); and 45 °C (◆). Curves were obtained by adjusting the experimental data by using eqs 6 and 7.

in the absence of CD were reasonably fit to single-exponential decay functions, whereas those in the presence of CD were fit to double exponential decay functions. Figure 3 depicts fluorescence intensity decay for a DEN/βCD solution at 5 °C. The single lifetime component, in the absence of CD, is obviously associated to the isolated DEN, τ_0 and it decreases as the temperature increases. In the presence of CD, the analysis of the profile decays were carried out by taking into account that the lifetime of the isolated DEN does not change upon CD addition. Therefore, one of the components of the decay is fixed to the short component lifetime (∼16−13 ns) obtained in the absence of CD at each temperature, τ_1 (= τ_0), and then, a second component τ_2 is obtained from the iterative reconvolution analysis.[43] τ_2, associated to the complexed form, is always longer than τ_1, and it remains almost constant with CD concentration but decreases with temperature. The proportion of the longest component relative to the shortest one increases upon addition of CD.

The bottom of Figure 2 shows the variation of the weighted average lifetime $<\tau>$ vs CD concentration for DEN and α- or βCD at different temperatures. Values of $<\tau>$ were obtained as

$$\langle\tau\rangle = \frac{\sum_i A_i \tau_i^2}{\sum_i A_i \tau_i} \qquad (1)$$

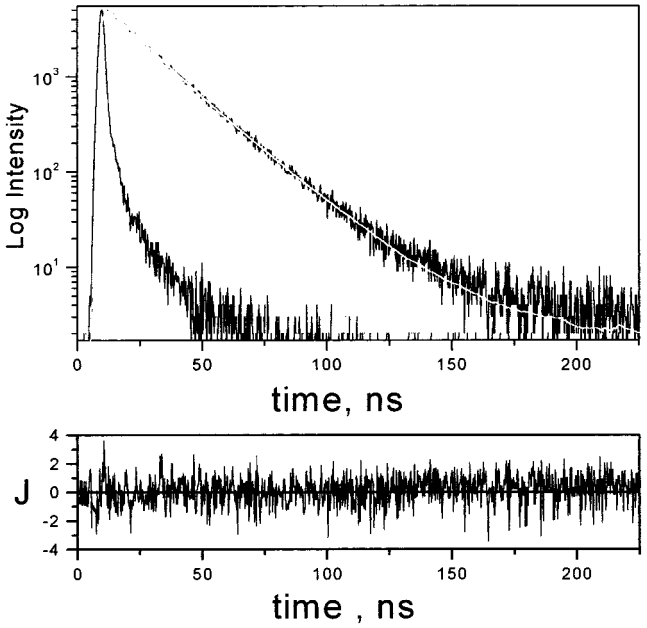

Figure 3. Time-dependent intensity decay for a DEN/βCD solution at 5 °C ([βCD] = 0.0130 M) upon selection of 385 nm as emission wavelength. Decay is fitted to a double exponential decay with lifetime components of τ_1 = 14.8 ns and τ_2 = 21.2 ns (χ^2 = 1.34).

where A_i is the preexponential factor of the component with a lifetime τ_i of the multiexponential function intensity decay. From the initial value in the absence of CD, (τ_0) $<\tau>$ increase monotonically with CD concentration, and it reaches a constant value, the lifetime for totally complexed DEN (τ_∞). As with R, through the plots, it can be predicted a negative enthalpy change during complexation.

2.3.3. Variation of R and <τ> upon Complexation. Emission spectra and fluorescence decay measurements of DEN in methanol/water, ethanol/water, and ethylene glycol/methanol mixtures at 25 °C in the absence of CD, were also performed. Methanol, ethanol, and water are solvents with relatively similar viscosity and different dielectric constants. Ethylene glycol and methanol have similar dielectric constant and they differ in viscosity. Thus, we can measure the change of both, the R and τ_0 parameters with polarity and viscosity almost independently. Emission spectra are similar to the ones obtained for water/CD solutions of DEN, but the ratio R changes with solvent mixture. Decay profiles in all cases can be fitted to single exponential decays ($<\tau>$ = τ_0). However, τ_0 depends on the mixture solvents. From these results, two facts are observed: (a) a decreasing of τ_0 and R is obtained, when measuring dilute solutions of DEN in methanol/water and ethanol/water mixtures, when medium polarity decreases, and (b) an increasing of τ_0, which hardly takes place for R, when measuring DEN in methanol/ethylene glycol mixtures, when medium viscosity increases. This indicates that, while R mainly depends on medium polarity, τ_0 is also sensitive, even more than to the polarity, to the medium microviscosity surrounding the DEN molecule. The inclusion process of DEN into a more hydrophobic CD cavity should be accompanied by a decrease of medium polarity and an increase of microviscosity. As a results $<\tau>$ and R should increase and decrease respectively upon complexation, as experimentally occurs.

2.3.4. Association Constants. For a G:CD$_n$ complex, with stoichiometry 1:n, whose global equilibrium can be done as

$$G + nCD \rightleftarrows GCD_n \qquad (2)$$

TABLE 1: Association Constants K, R_0 ($\langle\tau\rangle_0$) and R_∞($\langle\tau\rangle_\infty$), and Their Absolute Errors for DEN:αCD$_2$ and DEN:βCD$_2$ at Five Temperatures, Determined from Measurements of R and $\langle\tau\rangle$ (in parentheses) by Using Nonlinear Regression Fits from Eqs 6 and 7

DEN:αCD$_2$			
T,°C	$10^{-4}\times$ K, M^{-2}	R_0 ($\langle\tau\rangle_0$, ns)	R_∞ ($\langle\tau\rangle_\infty$, ns)
5	9.0 ± 0.8 (9.0 ± 2.0)	1.231 ± 0.007 (15.7 ± 0.2)	0.777 ± 0.008 (21.1 ± 0.2)
15	4.3 ± 0.2 (6.0 ± 1.0)	1.259 ± 0.003 (14.9 ± 0.1)	0.816 ± 0.006 (20.2 ± 0.2)
25	1.3 ± 0.3 (3.0 ± 1.2)	1.248 ± 0.005 (14.5 ± 0.2)	0.840 ± 0.040 (19.5 ± 0.6)
35	0.6 ± 0.2 (2.3 ± 1.1)	1.250 ± 0.003 (14.1 ± 0.2)	0.950 ± 0.070 (17.8 ± 0.6)
45	1.3 ± 0.8 (2.7 ± 0.5)	1.256 ± 0.005 (13.5 ± 0.1)	1.150 ± 0.030 (16.0 ± 0.2)
DEN:βCD$_2$			
T,°C	$10^{-4}\times$ K, M^{-2}	R_0 ($\langle\tau\rangle_0$, ns)	R_∞ ($\langle\tau\rangle_\infty$, ns)
5	12.9 ± 1.2 (17.0 ± 3.0)	1.225 ± 0.006 (14.9 ± 0.1)	0.760 ± 0.007 (20.2 ± 0.2)
15	7.2 ± 1.3 (11.0 ± 5.0)	1.237 ± 0.009 (14.5 ± 0.3)	0.798 ± 0.015 (19.5 ± 0.4)
25	2.7 ± 0.6 (4.0 ± 2.0)	1.238 ± 0.008 (14.6 ± 0.2)	0.820 ± 0.030 (18.7 ± 0.7)
35	1.4 ± 0.5 (2.1 ± 1.6)	1.233 ± 0.008 (13.4 ± 0.1)	0.89 ± 0.05 (16.6 ± 0.8)
45	1.4 ± 0.6 (1.5 ± 2.3)	1.247 ± 0.006 (12.9 ± 0.2)	1.0 ± 0.4 (15.1 ± 1.2)

the association constant can be written as

$$K = \frac{[\mathrm{G{:}CD}_n]}{[\mathrm{G}][\mathrm{CD}]^n} \tag{3}$$

Substituting the mass balance expressions for G and CD and assuming that the initial concentration of CD is $[\mathrm{CD}]_0 \gg [\mathrm{G{:}CD}_n] \gg [\mathrm{G{:}CD}_{n-1}]$... the molar fraction of complexed guest f_2 for equilibrium 2 can be written as

$$f_2 = \frac{K[\mathrm{CD}]_0^n}{1 + K[\mathrm{CD}]_0^n} \tag{4}$$

Such fraction f_2 can be evaluated from the steady state and from the decay measurements trough parameters such as R and the weighted average lifetime $\langle\tau\rangle$ previously defined as

$$f_2 = \frac{R_0 - R}{R_0 - R_\infty} = \frac{\langle\tau\rangle - \tau_0}{\tau_\infty - \tau_0} \tag{5}$$

where the symbols R_0 (τ_0), R_∞ (τ_∞), and R ($\langle\tau\rangle$) correspond to the defined properties for free (R or $\langle\tau\rangle$ at $[\mathrm{CD}]_0 = 0$), for complexed DEN (R or $\langle\tau\rangle$ at $[\mathrm{CD}]_0 = \infty$) and at a given CD concentration, respectively. From both eqs 4 and 5, the following can be obtained

$$R = \frac{R_0 + R_\infty \mathrm{K}[CD]_0^n}{1 + \mathrm{K}[CD]_0^n} \tag{6}$$

and

$$\langle\tau\rangle = \frac{\tau_0 + \tau_\infty K[\mathrm{CD}]_0^n}{1 + K[\mathrm{CD}]_0^n} \tag{7}$$

Equations 6 and 7 assume that R_0 and τ_0 are not affected upon the addition of CD. From eqs 4 and 5, a linear relation between $(R_0 - R)^{-1}$ or $(\langle\tau\rangle - \tau_0)^{-1}$ vs $[\mathrm{CD}]_o^{-n}$ can also be obtained. From such a representation the stability constant for the 1:n stoichiometry DEN:CD$_n$ complex can easily be obtained. However, the named double-reciprocal plots weigh more those ordinate values which have the largest errors. The nonlinear regression analysis from eqs 6 and 7 are sometimes more recommended. Solid lines depicted in Figure 2 are the results of these adjustments.[44] These fits reasonably correspond to 1:2 guest:host stoichiometries. Table 1 collects the equilibrium or association constants obtained from the nonlinear fits of both properties. Results are accompanied by larger experimental uncertainties than those obtained for DMN complexes[41] due to the lower values of the former constants, especially at the highest temperatures. The low fluorescence signal, due to the low DEN water solubility, also contributes to this uncertainty in the results. Due to intrinsic reasons of the method, time-resolved fluorescence measurements give larger uncertainties in K values as compared to the steady-state ones. At 25 °C, the average of association constants obtained from both methods were $(2.1 \pm 0.8) \times 10^4$ M^{-2} and $(3.4 \pm 1.3) \times 10^4$ M^{-2} for DEN:αCD$_2$ and DEN:βCD$_2$, respectively. These constants are considerably smaller than those for DMN:αCD$_2$, which is $(82 \pm 6) \times 10^4$ M^{-2} at the same temperature. These results indicate that at 25 °C, approximately 68% of DEN is complexed with a pair of αCDs and 77% does so with two βCDs when CD is added up to a concentration of 10^{-2} M. At this CD concentration more than 99% of DMN is complexed with two αCDs.

Constants K_1 and K_2 for each G + CD ⇄ GCD and GCD + CD ⇄ GCD$_2$ single steps can also be obtained. Equations 6 and 7 then can be modified as

$$R = \frac{R_0 + R_\infty \mathrm{K}_1[\mathrm{CD}]_0 + R_\infty \mathrm{K}_1\mathrm{K}_2[\mathrm{CD}]_0^2}{1 + \mathrm{K}_1[\mathrm{CD}]_0 + \mathrm{K}_1\mathrm{K}_2[\mathrm{CD}]_0^2} \tag{8}$$

and

$$\langle\tau\rangle = \frac{\tau_0 + \tau_\infty K_1[\mathrm{CD}]_0 + \tau_\infty K_1K_2[\mathrm{CD}]_0^2}{1 + K_1[\mathrm{CD}]_0 + K_1K_2[\mathrm{CD}]_0^2} \tag{9}$$

The results (not shown here), although they have uncertainties very close to their absolute values, reveal that $K_2 \gg K_1$ at any temperature for both DEN complexations with αCD or βCD, suggesting that most of the complexes formed have 1:2 stoichiometry. The fact that fluorescence intensity decays in the presence of CD at any temperature can reasonably be fitted to double exponential decays could corroborate it.

2.3.5. Polarity Surrounding DEN Guest. As the parameter R is very sensitive to the medium polarity, R_∞ can be used to get the dielectric constants, ϵ of the medium surrounding DEN. The procedure, used previously with other analogue guest molecules,[33,41] consists of obtaining a calibration curve of R vs ϵ by measuring R of DEN in mixtures of solvents with different polarities such as methanol/water and ethanol/water mixtures. R increases as the medium polarity increases and the dependence with ϵ is almost lineal. The equation that best fits the dependence

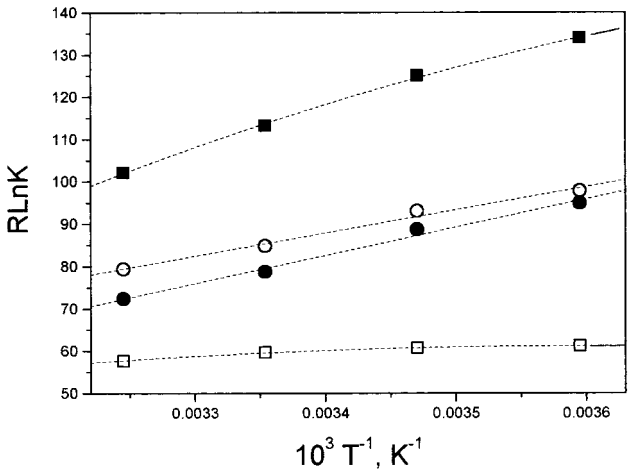

Figure 4. Van't Hoff plots for the formation of DEN:αCD$_2$ (●) DEN:βCD$_2$ (○), DMN:αCD$_2$ (■) and DMN:βCD (□).

TABLE 2: Values of the Enthalpy ($\Delta H°$) and Entropy ($-T\Delta S°$) Terms of the Complexation Processes

complex	ΔH°, kJ mol^{-1}	$-T\Delta S°$, kJK^{-1}mol^{-1}
DEN:αCD$_2$*	-45.3 ± 4.1	20.2 ± 4.2
DEN:βCD$_2$*	-46.6 ± 5.0	20.4 ± 4.9
DMN:αCD$_2$	-100.4 ± 1.6	66.5 ± 1.5
DMN:βCD	-13.4 ± 0.3	-4.4 ± 0.3

* Removing the data at 45 °C whose K values have large errors.

at 25 °C, is $R = 0.5503 + 0.0057\,\epsilon$ ($r = 0.991$). From the values of R_∞ collected in Table 1 at 25 °C, assuming that the DEN environment is relaxed when complexed, the estimated dielectric constant of the medium around DEN when is complexed with two α- or βCDs were ~50 and ~47, respectively. The latter value agrees with the one reported previously by other authors ($\epsilon \approx 48$)[25] and by us, $\epsilon \approx 49$[33] and 45.[41] However, the value of ~50 for αCD is much larger than the one obtained previously, $\epsilon \approx 10$[33] and 6.[41] This suggests that an important part of the guest DEN molecule could be exposed to the water polar solvent in the complex with αCD.

2.3.6. Enthalpy and Entropy Changes. The enthalpy and entropy changes upon complexation were obtained via van't Hoff plots from the data collected in Table 1. Figure 4 depicts van't Hoff plots from the association constant of both DEN 1:2 complexes obtained from steady state which are lineal in the range of our measurements. Table 2 shows the average of the values of enthalpy and the entropy term changes upon complexation obtained from both types of experiments. Associations are enthalpy driven. Results of $\Delta H°$ of both 1:2 complexes are very similar and, as usual, negative, but they differ from the one obtained for DMN:αCD$_2$, which is twice as large. Something similar occurs for $T\Delta S°$. For both complexes entropy terms are negative but quantitatively they are smaller, by a factor of 3, than those obtained for DMN:αCD$_2$. 1:2 complexes show absolute larger values of both terms than the ones obtained for the 1:1 DMN:βCD complexes. Entropy, however, has opposite sign. Thus, the value of $\Delta H° < 0$ for the formation of the 1:2 DEN:CD complexes is typical of hydrophobic species whose complexation is driven by van der Waals interactions, perhaps hydrogen bonding or any other attractive interaction which makes enthalpy decrease during the process. The loss of entropy ($\Delta S° < 0$) will however be due to the balance of a positive contribution from the loss of the ordered water molecules that solvates the free guest and a negative one due to the loss in freedom degrees of the whole system.

3. Molecular Mechanics Calculations

3.1. Methods. The calculations were performed with Sybyl 6.6[46] using the Tripos Force Field.[47] The total potential energy of a system was obtained as the sum of six contributions, bond stretching, angle bending, torsion, van der Waals, electrostatics, and out-of-plane. A relative permittivity of 3.5 in vacuo and a lineal function of the distance in the presence of water were used.[41] DEN and water molecule charges were obtained by MOPAC.[47] CD$_S$ and water charges were the same as used in previously.[34,36,41] Nonbonded cutoff distances were set at 8 Å. Minimization of the of the system was performed by the simplex algorithm and the conjugate gradient was used as a termination method (gradients 0.2 and 3.0 kcal/molÅ in vacuo and in water respectively).[48,49] Solvation was performed by the Molecular Silverware[50] algorithm (MS). PBC conditions were employed using a cubic box with side of 31.62 Å (32.12 Å) for 1:1 and a box of dimensions 37.13 Å ×31.47 Å ×31.47 Å (37.65 Å ×32.15 Å ×32.15 Å) for 1:2 complexes with αCD (βCD).

Binding energy, $E_{binding}$ (G:H) for the (1:1) G:H complex (G = guest, H = host), which is associated to the enthalpy change, was obtained as the difference between the potential energy of the complex and the sum of the potential energies of the isolated DEN and CD in the same conformation as

$$E_{binding,G:H} = E_{G:H} - (E_G + E_H) \tag{10}$$

In a similar manner, for the 1:2 complexes, two different binding energies named $E_{binding,\ G:H1-H2}$ and $E_{binding,\ G-H1+H2}$ were calculated. Any nonbonded contributions can be obtained in the same way. The change of energy (or any contribution) upon complexation is obtained by

$$\Delta E = E_{min} - E_\infty \tag{11}$$

where E_∞ and E_{min} are the values of such energy at an infinite G−H distance and at the structure of minimum $E_{binding}$. The strain energy of CDs is the sum of torsional, stretching and bending energies. A hydrogen bond is assumed when the distance between the hydrogen (H), bonded to a donor (D), and the acceptor (A) is between 0.8 and 2.8 Å and the angle D−H−A is larger than 120°.

3.2. Initial Conformations and Emulation of the Complexation. The initial structure of the α- and βCDs were in the nondistorted form.[34−41] To get the initial conformation of DEN a Molecular Dynamic (MD) simulation of 1 ns in the vacuum at 300 K was performed. Characteristics of the MD simulation were similar to others reported.[51] From the 5000 conformations analyzed, the five conformations with the smallest energies were selected and then optimized. The most stable, as expected, was a conformation where the ester groups were in the same plane of the naphthalene ring, the dipole moments oriented in opposite directions and the ethyl group close to the all-trans conformation, as depicted in Figure 5.

The schemes for the 1:1 and 1:2 complexation processes are depicted in Figure 5. Details of the emulation where similar to the ones described previously.[41] In brief, the origin of coordinates, O was placed at the center of mass of the CD glycosidic oxygen atoms. The y axis refers to the n-fold rotation CD axis and the z axis passes through one of the n glycosidic oxygens placed in the xz plane. The inclusion angle θ defines the angle between yz and the DEN naphthalene ring planes. The OO′C-(9) angle, δ defines the orientation of the DEN relative to y axis. The host−guest distance was measured as the OO′ distance. For the 1:1 complexation process the DEN was

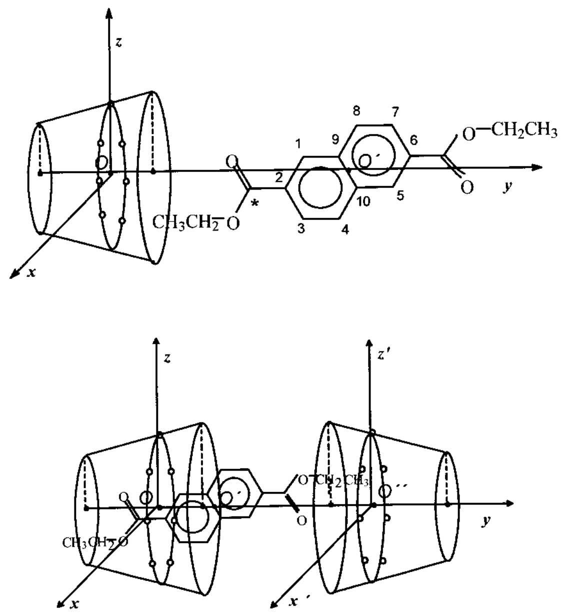

Figure 5. Scheme for the 1:1 (top) and 1:2 (bottom) DEN:host complex formation.

approached in small steps along the y axis. The 1:2 complexation process was emulated, in a similar way, by incrementally approaching a second CD (head-to-head) to the previously formed 1:1 complex (minimum binding energy structure) according to the scheme depicted at the bottom of Figure 5. The distance between CDs is defined by the OO″ distance along the y axis. The association angle θ', which initially fixed at 0°, is measured by the dihedral angle O(*4*)−O′−O″−O(*4″*), where O(*4*), O(*4″*) are glycosidic oxygens of both CDs. θ and θ' angles slightly change upon association from the initial values.

First, the most favorable δ was estimated. For this purpose, $E_{\text{binding},\text{DEN:CD}}$ for the conformations generated by scanning θ from 0 to 60° at 5° intervals, the OO′ distance from 16 to − 4 Å at 2 Å intervals and δ from 50° to 130° at 40° increment were obtained. Critical examination of the results gives δ around 70° and 60° for αCD and βCD approaching. In a second step, $E_{\text{binding},\text{DEN:CD}}$−OO′ distance−$\theta$ 3D-plots, where δ were fixed at the previous values, were obtained. Analysis of these plots shows the possible trajectories of the smallest binding energies. These are obtained for the δ and θ pairs of ∼70°, ∼40° and ∼60°,∼55° when DEN approaches the α- and βCD, respectively. These angles were used for the initial structures. Up to here the calculations were in vacuo, the remaining ones were performed in the presence of water.

3.3 (1:1) DEN:CD Complexes. The DEN was approached to each CD from $y = 16$ (Å) to $y = -4$ (Å) at 0.5 (Å) intervals and subsequentely each structure generated was solvated and then minimized. The top of Figure 6 depicts E_{binding} together with van der Waals and electrostatic contributions (at the bottom) for DEN-αCD and DEN-βCD inclusion processes. E_{binding} for the inclusion of DEN with βCD curves does not show large gaps indicating that DEN can penetrate into the cavity without having large energy barriers. In contrast, inclusion with αCD is accompanied by large gaps with $E_{\text{binding}} > 0$, which would require a relatively large amount of energy to surmount it. According to this, structures of minima values of binding energies are reached for $y = +7.8$ (Å) and $+2.7$ (Å) and δ_{min}, θ_{min} angle pairs of approximately 65°,40° and 63°, 58° for DEN:αCD and DEN:βCD complexes, respectively. In both cases, an important portion of DEN is placed outside the CD cavity. Figure 6 depicts the limits (primary and secondary oxygen rim)

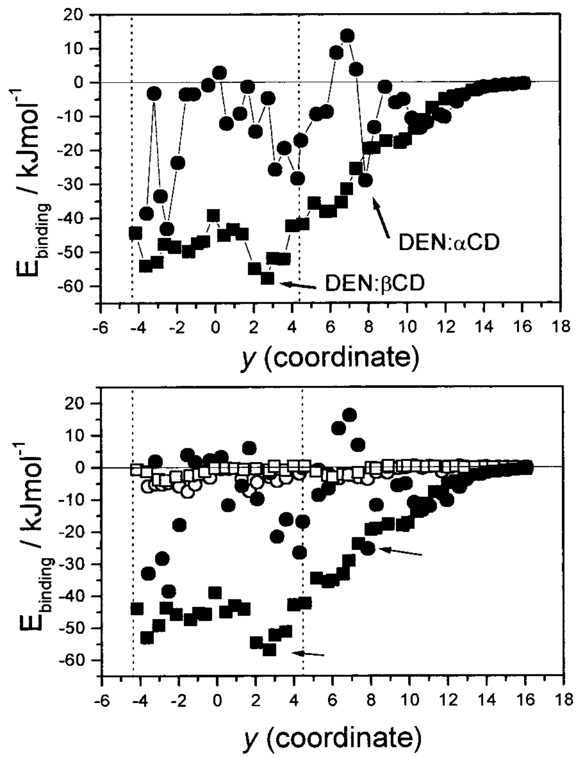

Figure 6. Top: Binding energy vs y coordinate (Å) in water for DEN:αCD (●) and DEN:βCD (■). Bottom: van der Waals (filled symbols) and electrostatic (open symbols) contributions to binding energy for DEN:αCD (circles) and DEN:βCD (squares).

of the initial nondistorted CDs of 8.81 Å depth by dashed lines. For DEN:αCD the center of mass of the naphthalene group is far away from the CD cavity, whereas for DEN:βCD it is slightly inside. The bottom of Figure 6 shows that most of the stabilization of both 1:1 complexes comes from van der Waals interactions. Columns 2 and 3 of Table 3 collects the variation of binding energy and other contributions upon 1:1 complexation of DEN obtained by eq 11. Most of the stabilization of 1:1 complexes (88% and 98% for α- and βCD respectively) comes from van der Waals nonbonded contributions. As collected in Table 3, the DEN:αCD formation is accompanied by an increase of total potential energy, whereas DMN:βCD is followed by a slight decrease of such energy. This is mainly due to the increase in both, the CD macroring and the DEN strains, which is much larger for the process of inclusion of DEN into αCD than into βCD. van der Waals interactions are mainly responsible for the variation of total potential energy for the structures of minimum binding energies, of which the most important contribution is due to host−guest nonbonded interactions. Thus, the pair DEN-αCD experiences a slight increase in van der Waals energy upon complexation, whereas DEN-βCD shows a decrease. These conclusions can also be inferred from Figure 7, which exhibits the variation of total potential energy and different contributions of the complex during the approaching of DEN to the CD. Although quantitatively van der Waals interactions are the smallest contribution to the total potential energy, they are responsible for the larger stabilization of 1:1 DEN:βCD complexes than its counterpart.

3.4. DEN:CD$_2$ Complexes. The top of Figure 8 exhibits the change in E_{binding} [G−(H1 + H2)] with the distance between CDs, i.e., the binding energy between DEN and two CD hosts during the approaching of a second CD (H2) to the (1:1) DEN:CD complex of minimum E_{binding} obtained previously, according to the process emulated at the bottom of Figure 5. Binding

TABLE 3: Variation in Binding Energies and Selected Components between the Minimum Energy and at the Largest Separation of the Two Components (considered as infinite distance) for the Formation of 1:1 and 1:2 DEN−CD Complexes in the Presence of Water

energy, kJ.mol^{-1}	DEN: αCD	DEN: βCD	energy, kJ.mol^{-1}	DEN: αCD_2	DEN: βCD_2
$E_{binding}$	−28.4	−57.3	$E_{binding}$[G−(H1+H2)]	−35.8	−39.1
electrostatic	−3.6	−0.9	electrostatic	−0.9	−8.5
van der Waals	−24.9	−56.4	van der Waals	−34.9	−30.6
E_{tot} for *G:H1*	+43.6	−48.7	$E_{binding}$ [(G:H1)−H2]	−34.0	−71.8
electrostatic	−7.1	−5.0	electrostatic	−0.5	−60.6
van der Waals	+2.8	−53.0	van der Waals	−33.7	−11.2
E_{tot} for *H1*	+45.1	+4.4	$E_{binding}$ [H1−H2]	−0.6	−13.7
electrostatic	−3.4	−3.9	electrostatic	0.7	−55.9
van der Waals	+20.1	−4.1	van der Waals	−1.2	42.2
strain	+28.4	+12.2	E_{tot} for *G:H1H2*	60.1	517.9
E_{tot} for *G*	+27.0	+4.4	electrostatic	16.2	58.2
electrostatic	−0.2	−0.2	van der Waals	−42.7	225.7
van der Waals	+7.7	+7.5	strain	86.7	234.1
strain	+19.1	+2.4			

(G = DEN guest; H1 = CD host in the 1:1 complex; H2 = second CD host added to form the 1:2 complex).

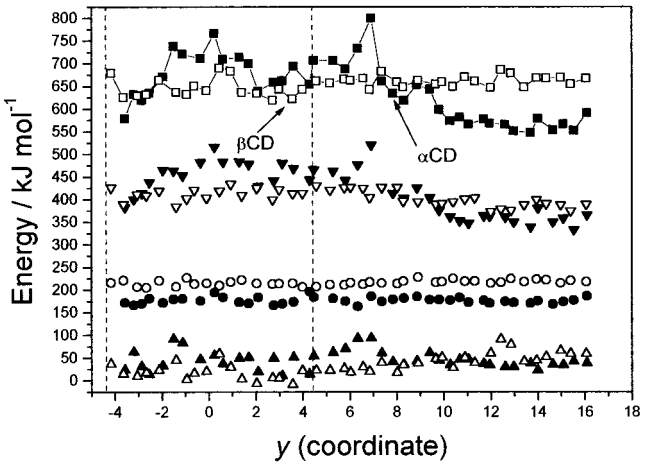

Figure 7. Different contributions to the total potential energy of the solvated conformations (squares), as a function of the OO′ distance along *y* coordinate, for 1:1 DEN complexes with αCD (filled symbols) and βCD (open symbols). The contributions are: van der Waals (up triangles), electrostatic (circles), and strain (down triangles). Arrows point out structures of minima $E_{binding}$ and dashed lines show the limits of the nondistorted CD torus (depth is 8.81 Å).

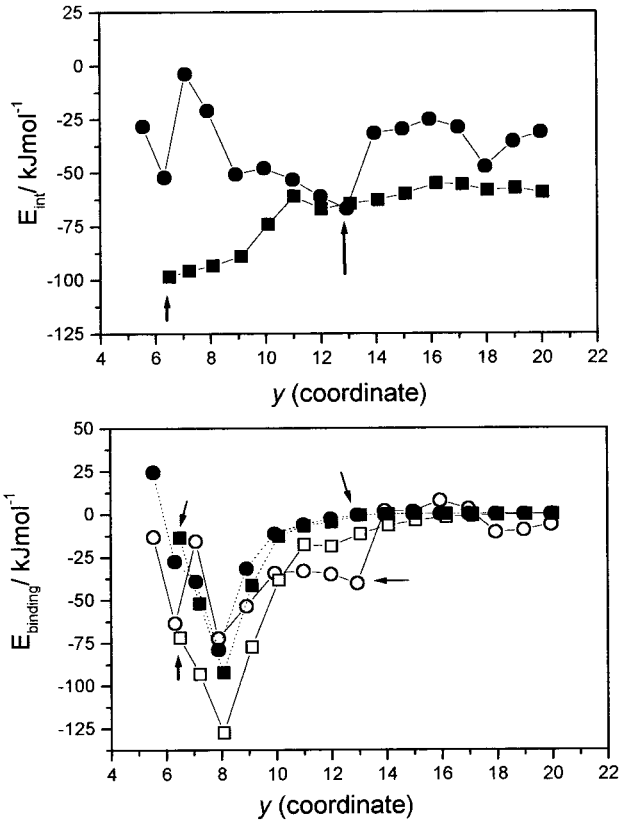

Figure 8. Top: $E_{binding}$ [G−(H1 + H2)] as a function of the distance between αCDs (●) or βCDs (■) hosts along the *y* coordinate, for the formation of 1:2 complexes in the presence of water. Bottom: $E_{binding}$ [(G:H1) − H2)] (filled symbols) and $E_{binding}$ [H1 − H2)] (open symbols) as a function of the distance between αCDs (circles) or βCDs (squares).

energies upon formation of 1:2 complexes seem to decrease, reaching a minimum value. Structures of minimum values of $E_{binding}$ are accomplished at *y* coordinates for the centers of mass of H2 (O″) and naphthalene group (O′) of +12.9 (Å) and +8.0 (Å) for DEN:αCD_2 (−66.9 kJ mol^{-1}) and of +6.5 (Å) and +2.7 (Å) for DEN:βCD_2 (−98.5 kJ mol^{-1}). The bottom of Figure 8 also depicts two interaction energies, $E_{binding}$[(G:H1) − H2)] and $E_{binding}$[H1 − H2] vs the distance OO″ between CDs. The decreasing of both energies as the H1−H2 distance decreases indicates that the formation of both 1:2 stoichiometries complexes are favorable. Table 3 also collects the changes in the three types of binding energies and different contributions upon complexation, together with the total potential energy change of the whole complex. The most important feature of these results is the negative large contribution of the electrostatic interactions to $E_{binding}$[(G:H1) −H2)] and $E_{binding}$[H1 − H2] for the complex with βCD. For the structure of minimum binding energy, the centers of both βCDs (αCDs) are separated by ∼6.5 Å (∼13 Å). The distance is short enough to give a van der Waals nonbonded repulsive interaction between βCDs (and even a relatively large strain of both macrorings), but adequate to βCDs secondary hydroxyl groups to interact giving a large negative nonbonded electrostatic interaction. Most of this contribution must arise from the presence of intermolecular hydrogen bonds (HB) between βCDs. A total of 10 βCDs intermolecular hydrogen bonds could be possible for the most stable structure of DEN:βCD_2, which is depicted in Figure 9. The DEN:αCD_2 complex, however, shows negative van der Waals nonbonded and almost insignificant electrostatic interactions. The distance between αCDs is large enough to avoid the formation of intermolecular HBs. The top of Figure 9 depicts the most stable structure of the DEN:αCD_2 complex. The αCDs do not shield the DEN from the solvent as it was in the DEN:βCD_2 complex. The structures of both complexes could agree with the estimated dielectric constants of ∼50 and ∼47 of the medium surrounding DEN when it is complexed with a pair of α- or βCD_s

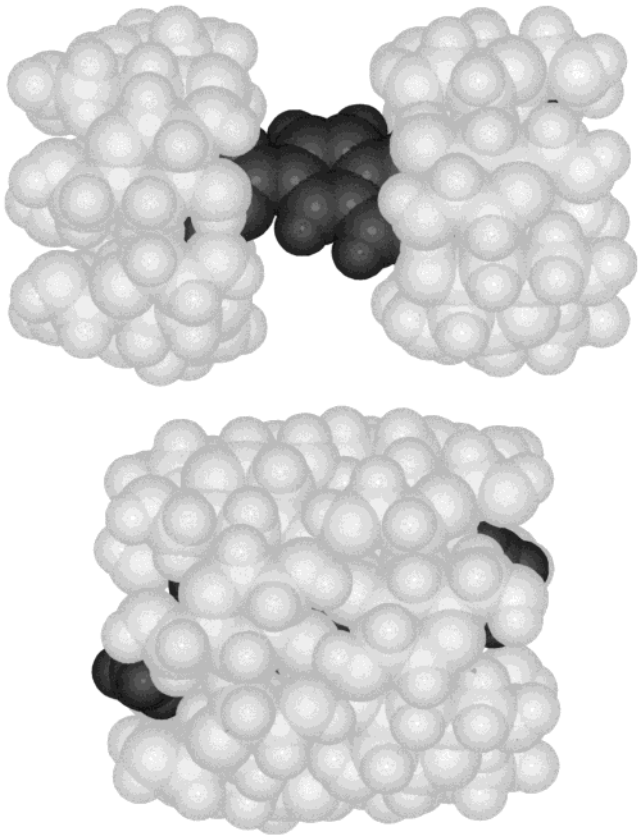

Figure 9. Structures of minimum binding energy for DEN:CD_2 complexes with α- (top) and *β*CD (bottom). Water molecules were removed.

respectively. In fact the latest value is the polarity of the inner *β*CD cavity. The value of 50 is much larger than the dielectric constant estimated for the αCD cavity (∼10),[33,41] because part of DEN is in contact with water. The difference in the structures, however, cannot explain that both entropy terms are similar for both complexes. Anyway, results show that the unfavorable sign of entropy is mainly due to the loss of degrees of rotational and translational freedom during the process.

4. Conclusions

The DEN guest forms complexes with α- and *β*CDs with stoichiometries 1:2. The stability of DEN:*β*CD_2 complex is slightly larger than the one for DEN:αCD_2. Both complexes, however, show smaller stability than the DMN:αCD_2 complex. The geometry of DEN:αCD_2 and DEN:*β*CD_2 is rather different. In the latter complex, DEN is perfectly shielded from the solvent, whereas in the former one part of the guest is in contact with water. As a results the polarity of the medium surrounding DEN is considerably higher than the one estimated for the inner αCD cavity. Molecular Mechanics prove the viability of the 1:2 stoichiometry complex formation. The nonbonded van der Waals interactions are mainly responsible for the stability of both complexes. Addition of a second *β*CD to the 1:1 DEN:*β*CD complex, nevertheless, is accompanied by favorable electrostatics nonbonded interactions, mostly due to hydrogen bonding between *β*CDs, which does not take place for the formation of DEN:αCD_2. This could also be the reason for the higher stabilization of DEN:*β*CD_2 complex than its counterpart. Both 1:2 complex formations are exothermic and enthalpy driven with favorable nonbonded guest−host van der Waals interactions and hydrogen bonding between CDs that favor $\Delta H < 0$. The negative entropy change can be attributed to the overall loss of freedom motion over the certain disorder that accompanies the loss of water molecules surrounding the hydrophobic guest.

Acknowledgment. This research was supported by CICYT Grant No. PB97-0778. We wish to express our thanks to M.L. Heijnen for assistance with the preparation of the manuscript.

References and Notes

(1) Szejtli, J.; Osa, T. *Comprehensive Supramolecular Chemistry*; Elsevier: Oxford, 1996; Vol. 3, Cyclodextrins.
(2) D'Souza, V. T.; Lipkowitz, K. B. *Chem. Rev.* **1998**, *98*(5), 1741.
(3) Harada, A. *Adv. Polym. Sci*. **1997**, *133*, 141.
(4) Harada, A.; *Acc. of Chem. Res.* **2001**, *34*(6), 456.
(5) Yorozu, T.; Hoshino, M.; Imamura, M.; Shizuka, H. *J. Phys. Chem.* **1982**, *86*, 4422.
(6) Nakajima, A. *Spectrochim*. **1983**, *Acta 39A (10)*, 913.
(7) Patonay, G.; Shapira, A.; Diamond, P.; Warner, I. M. *J. Phys. Chem.* **1986**, *90*, 1963.
(8) Agbaria, R. A.; Uzan, B.; Gill, D. *J. Phys. Chem.* **1989**, *93*, 3855.
(9) Takahashi, K. *J. Chem. Soc. Chem. Commun.* **1991**, 929.
(10) Flamigni, L. *J. Phys. Chem.* **1993**, *97*, 9566.
(11) Monti, S.; Köhler, G.; Grabner, G. *J. Phys. Chem.* **1993**, *97*, 13 011.
(12) Schuette, J. M.; Warner, I. M. *Talanta* **1994**, *41*(5), 647.
(13) Fraiji, E. K. Jr.; Cregan, T. R.; Werner, T. C. *Appl. Spectrosc.* **1994**, *48*(1), 79.
(14) Nakamura, A.; Sato, S.; Hamasaki, K.; Ueno, A.; Toda, F. *J. Phys. Chem.* **1995**, *99*, 10 952.
(15) Nelson, G.; Patonay, G.; Warner, I. M. *Appl. Spectrosc.* **1987**, *41*(7), 1235.
(16) Kobayashi, N.; Saito, R.; Hino, H.; Hino, Y.; Ueno, A.; Osa, T. *J. Chem. Soc. Perkin. Trans. 2.* **1983**, 1031.
(17) Turro, N. J.; Okubo, T.; Weed, G. C. *Photochem. Photobiol.* **1982**, *35*, 325.
(18) Kano, K.; Takenoshita, I.; Ogawa, T. *Chem. Lett. Chem. Soc. Jpn.* **1982**, 231.
(19) Hamai, S. *Bull. Chem. Soc. Jpn*. **1982**, *55*, 2721.
(20) Hamai, S. *J. Phys. Chem.* **1989**, *93*, 6527.
(21) Catena, G. C.; Bright, F. V. *Anal. Chem.* **1989**, *61*, 905.
(22) Yorozu, T.; Hoshino, M.; Imamura, M. *J. Phys. Chem.* **1982**, *86*, 4426.
(23) Hashimoto, S.; Thomas, J. K. *J. Am. Chem. Soc.* **1985**, *107*, 4655.
(24) Nakajima, A. *Bull. Chem. Soc. Jpn*. **1984**, *57*, 1143.
(25) Street, K. W. Jr.; Acree, W. E. Jr. *Appl. Spectrosc.* **1988**, *43*(7), 1315.
(26) Muñoz de la Peña, A.; Ndou, T. T.; Zung, J. B.; Warner, I. M. *J. Phys. Chem.* **1991**, *95*, 3330.
(27) Muñoz de la Peña, A.; Ndou, T. T.; Zung, J. B.; Greene, K. L.; Live, D. H.; Warner, I. M. *J. Phys. Chem.* **1991**, *95*, 1572.
(28) Will, A. Y.; Muñoz de la Peña, A.; Ndou, T. T.; Warner, I. M. *Appl. Spectrosc.* **1993**, *47*(3), 277.
(29) Kusumoto, Y. *Chem. Phys. Lett.* **1987**, *136*, 535.
(30) Edwards, H. E.; Thomas, J. K. *Carbohydr. Res.* **1978**, *65*, 173.
(31) Sherrod, M. J. In S*pectroscopic and Computational Studies of Supramolecular Systems*; Davies, J. E. D., Ed.; Kluwer Academic Publishers: Dordrecht, The Netherlands, 1992; p 187.
(32) D'Souza, V. T.; Lipkowitz, K. B. *Chem. Rev.* **1998**, *98*(5), 1829.
(33) Madrid, J. M.; Mendicuti, F. *Appl. Spectrosc.* **1997**, *51*, 1621.
(34) Madrid, J. M.; Pozuelo, J.; Mendicuti, F.; Mattice, W. L. *J. Colloid Interface Sci.* **1997**, *193*, 112.
(35) Pozuelo, J.; Mendicuti, F.; Mattice, W. L. *Macromolecules* **1997**, *30*, 3685.
(36) Madrid, J. M.; Mendicuti, F.; Mattice, W. L. *J. Phys. Chem B.* **1998**, *102*, 2037.
(37) Pozuelo, J.; Mendicuti, F.; Mattice, W. L. *Polym. J.* **1998**, *30*, 479.
(38) Madrid, J. M.; Villafruela, M.; Serrano, R.; Mendicuti, F. *J. Phys. Chem B.* **1999**, *103*, 4847.
(39) Pozuelo, J.; Nakamura, A.; Mendicuti, F. *J. Incl. Phenom. and Macroc. Chem*. **1999**, *35*(3), 467.
(40) Pozuelo, J.; Mendicuti, F.; Saiz, E. In *Proceedings of the 9th International Symposium on Cyclodextrins*; Labandeira, J. J., Vila, J. L., Eds.; Kluwer Academic Publishers: The Netherlands, 1999; p 567.
(41) Cervero, M.; Mendicuti, F. *J. Phys. Chem B.* **2000**, *104*, 1572.
(42) Martin, O.; Mendicuti, F.; Saiz, E.; Mattice, W. L. *J. Polym. Sci.: Part B: Polym Phys.* **1999**, *37*, 253.
(43) O'Connor, D. V.; Ware, W. R.; André, J. C. *J. Phys. Chem.* **1979**, *83*, 1333.
(44) MicroCal Origin, 5.0, MicroCal Software, Inc.: Northampton, MA.
(45) Sybyl 6.6. Tripos associates, St. Louis, Missouri, USA.

(46) Crark, M.; Cramer, R. C. III.; van Opdenbosch, N. *J. Comput. Chem.* **1989**, *10*, 982.
(47) MOPAC-AM1, included in the Sybyl 6.6 package.
(48) Brunel, Y.; Faucher, H.; Gagnaire, D.; Rasat, A. *Tetrahedron* **1975**, *31*, 1075.
(49) Press, W. H.; Flannery, B. P.; Teukolski, S. A.; Vetterling, W. T. *Numerical Recipes: The Art of Scientific Computing*; Cambridge University Press: 1988; p 312.
(50) Blanco, M. *J. Comput. Chem.* **1991**, *12*, 237.
(51) Junquera, E.; Mendicuti, F.; Aicart, E. *Langmuir* **1999**, *15*(13), 4472.